Thermalization of Orbital Angular Momentum Beams in Multimode Optical Fibers

E. V. Podivilov,[1,2,†] F. Mangini,[3,4,†,*] O. S. Sidelnikov,[1] M. Ferraro,[4] M. Gervaziev,[1] D. S. Kharenko,[1,2] M. Zitelli,[4] M. P. Fedoruk,[1] S. A. Babin,[1,2] and S. Wabnitz[1,4]

[1]*Novosibirsk State University, Novosibirsk 630090, Russia*

[2]*Institute of Automation and Electrometry SB RAS, 1 academician Koptyug avenue, Novosibirsk 630090, Russia*

[3]*Department of Information Engineering, University of Brescia, Via Branze 38, 25123 Brescia, Italy*

[4]*Department of Information Engineering, Electronics, and Telecommunications, Sapienza University of Rome, Via Eudossiana 18, 00184 Rome, Italy*

(Received 28 December 2021; revised 20 April 2022; accepted 31 May 2022; published 17 June 2022)

We report on the thermalization of light carrying orbital angular momentum in multimode optical fibers, induced by nonlinear intermodal interactions. A generalized Rayleigh-Jeans distribution of asymptotic mode composition is obtained, based on the conservation of the angular momentum. We confirm our predictions by numerical simulations and experiments based on holographic mode decomposition of multimode beams. Our work establishes new constraints for the achievement of spatial beam self-cleaning, giving previously unforeseen insights into the underlying physical mechanisms.

DOI: 10.1103/PhysRevLett.128.243901

Statistical physics has been traditionally and successfully employed to describe the average properties of a large ensemble of particles, whose interactions are governed by classical mechanics. This approach lies at the basis of thermodynamics, whose laws determine the macroscopic properties of matter, that evolve in a low-dimensional or reduced phase space. Subsequently, the thermodynamic approach has been extended to describe the statistical evolution of a large number of classical electromagnetic waves, analogously to bosonic systems, such as superconductors and superfluids [1–5]. Thermalization effects have been explored in different photonic platforms, ranging from disordered lattices to plasmonic systems [6–8].

Peculiar is the case of multimode optical fibers (MMFs), which are an excellent test-bed for classical wave condensation phenomena. Indeed, Bose-Einstein condensation of fiber modes has been demonstrated in graded-index (GRIN) MMFs [9], and it can be theoretically described by a model based on a weak wave turbulence approach [10]. Whereas a general model of thermalization of light in multimode systems has been recently introduced, showing that the average number of photons in each mode of the fiber obeys a Rayleigh-Jeans (RJ) distribution [11,12]. Because of the role of high-order modes at the occurrence of thermal equilibrium in MMFs, thermalization of a multimode field is a more general situation than condensation [12].

On the other hand, experimental observations have revealed that, as the input power of a laser beam coupled into a GRIN MMF grows above a certain threshold, the intensity speckles generated by multimode interference may spontaneously reorganize into a bell-shaped beam, which approaches the fundamental mode of the fiber [13,14]. This spatial self-organization effect is known as beam self-cleaning (BSC) [15], and it has similarities with wave condensation in hydrodynamic 2D turbulent systems [16]. Since its first demonstration, BSC has been extensively experimentally studied [16–23], in order to fully clarify its physical mechanism. All of the studies reported so far in the literature agree on the fact that modal four-wave-mixing (FWM) interactions are crucial for activating BSC. The fraction of energy in the fundamental mode has been verified to obey the expected dependence on the initial degree of spatial correlation [17], or on the internal energy of the input beam with a fixed power value [9].

As a thermodynamic phenomenon, BSC can be seen as the tendency of the optical beam to experience an irreversible evolution toward a state of thermal equilibrium, which is established by conservation laws. Specifically, the total number of photons, the total energy, and the total momentum of motion must be simultaneously conserved [9,12].

As a matter of fact, another quantity is conserved when a beam of light propagates in waveguide systems: its total orbital angular momentum (OAM). First introduced by Allen *et al.* in 1992 [24], interest in OAM beams has increased tremendously, thanks to their widespread potential for applications. These range from telecommunications [25] to quantum optics [26], holography [27], astronomy [28], and optical tweezers [29,30]. To date, BSC has only been observed with laser beams that carry no OAM.

In this Letter, we extend current knowledge by describing, both theoretically and experimentally, the thermalization of OAM-carrying multimode beams in nonlinear optical fibers. We present a general theory of thermalization of light in a MMF, which, at variance with previous

literature [11,31], takes into account the conservation of the OAM. This permits one to derive a generalized RJ distribution for the relative occupation of the fiber modes, which directly stems out of the conservation laws that rule the FWM process in MMFs. Remarkably, our model shows that BSC, as a result of beam thermalization, can only be achieved by means of laser beams which do not carry any OAM. Theoretical predictions are then compared to numerical simulations, which turn out to be in excellent agreement. Finally, we carried out an experimental characterization of the thermal mode distribution at the fiber output, based on a holographic mode decomposition (MD) technique [32]. In our implementation, OAM is imparted to an input Gaussian laser beam by means of properly adjusting its coupling condition into the fiber [33].

In our theoretical model, we decompose the amplitude (A) of a light pulse in a GRIN MMF in terms of the real normalized *radial* OAM eigenfunctions $F_{\ell,m}$, so that

$$A(t,z,r,\phi)=\sum_{k,\ell,m}A_{\ell,m}(\omega_k,z)e^{i\omega_k t-ip_{\ell,m}(\omega_k)z+im\phi}F_{\ell,m}(r), \tag{1}$$

and $2\pi\int_0^\infty rdr[F_{\ell,m}(r)]^2=1$. Here, $p_{\ell,m}(\omega_k)$ and $A_{\ell,m}(\omega_k,z)$ are the propagation constant and the slowly varying amplitude of a mode with radial index ℓ, azimuthal index m, and frequency $\omega_k=\omega_0+2\pi Hk$, where ω_0 is the carrier frequency and H is the pulse repetition rate. In the Supplemental Material [34], we outline the transformation from the conventional Laguerre-Gauss basis to the OAM basis, and we show that the OAM modes are the well-known vortex beams.

Although BSC is a purely spatial effect, its high threshold powers have required the use of pulsed sources for its observation. Moreover, it has been shown that BSC is accompanied by significant temporal pulse reshaping [35], which may be associated with a transfer of disorder between spatial and temporal degrees of freedom [36]. For this reason, in our derivation, we keep explicit the dependence of the light amplitude on frequency ω_k.

Let us normalize $|A(t,z,r,\phi)|^2$ to the beam intensity, so that for each mode (ℓ,m) and frequency component ω_k we may introduce the average power $W_{k,\ell,m}(z)=|A_{\ell,m}(\omega_k,z)|^2$, the mode energy in a pulse $E_{k,\ell,m}(z)=W_{k,\ell,m}(z)/H$, the number of photons $N_{k,\ell,m}(z)=E_{k,\ell,m}(z)/\hbar\omega_k$, the longitudinal component of pulse momentum of motion $P_{k,\ell,m}(z)=p_{\ell,m}(\omega_k)N_{k,\ell,m}(z)$, and the OAM $M_{k,\ell,m}(z)=\hbar mN_{k,\ell,m}(z)$. There are four conservation laws in the FWM process. Specifically, the total energy of each pulse $E=\sum_{k,\ell,m}E_{k,\ell,m}(z)=\text{const}$, the number of photons in each pulse $N=\sum_{k,\ell,m}N_{k,\ell,m}(z)=\text{const}$, the longitudinal component of the momentum of motion of a pulse $P=\sum_{k,\ell,m}P_{k,\ell,m}(z)=\text{const}$, and the longitudinal component of the pulse OAM $M=\sum_{k,\ell,m}M_{k,\ell,m}(z)=\text{const}$. All of the conserved quantities (E, N, P, and M) are fully defined by the injection conditions of the laser beam into the fiber whereas, during propagation, FWM leads to energy exchange between fiber modes, similarly to particle collisions in a gas, thus shuffling the values of $N_{\ell,m,k}(z)$. One could expect then that the photon system reaches thermodynamic equilibrium over a finite time (i.e., a finite distance, say, z^*), whenever each elementary FWM process leading to energy transfer into some modes is equally probable as its reverse process. In this case, for $z>z^*$, the statistics of an ideal photon gas is described by the Boltzmann distribution.

At $z>z^*$, this leads to a RJ distribution for the number of photons $N_{k,\ell,m}=(T/\hbar\omega'_{k,\ell,m}-\mu)$ occupying the mode (k,ℓ,m) in the coordinate system moving with the light pulse at speed V, and rotating with its angular velocity Ω [37]. Here, T is the *statistical* temperature of photons in a light pulse (which is analogous to the temperature of electrons in particle accelerator electron beams), μ is the chemical potential, $\omega'_{k,\ell,m}=\gamma(\omega_k-Vp_{\ell,m}-\Omega m)$, $\gamma=1/(1-V^2/c^2)^{1/2}\simeq\sqrt{2}$ is a relativistic factor, and c is the speed of light in vacuum. At thermal equilibrium, the number of photons occupying mode (ℓ,m) with frequency ω_k in a laboratory reference system reads as

$$N_{k,\ell,m}=\frac{T/\sqrt{2}}{\hbar\omega_k-\frac{\mu}{\sqrt{2}}-\hbar Vp_{\ell,m}-\hbar\Omega m}, \tag{2}$$

which is a generalized form of the RJ distribution. It is worth noting that Eq. (2) can be equivalently derived starting from conservation laws, without recurring to the change of coordinate system (see the Supplemental Material [34]).

FWM scattering of waves must obey the conservation laws of E, N,P, and M, which lead to the following conditions:

$$\omega_1+\omega_2=\omega_3+\omega_4, \tag{3}$$

$$p_{\ell_1,m_1}(\omega_1)+p_{\ell_2,m_2}(\omega_2)=p_{\ell_3,m_3}(\omega_3)+p_{\ell_4,m_4}(\omega_4), \tag{4}$$

$$m_1+m_2=m_3+m_4, \tag{5}$$

where ℓ_i, m_i, and ω_i with $i=1,2,3,4$ characterize each of the four waves. If any of Eqs. (3), (4), or (5) is not satisfied, the scattering process is forbidden, the ergodicity hypothesis fails, and the multimode optical system never reaches its thermodynamic equilibrium.

Let us consider the FWM of narrow spectrum beams, i.e., $|\omega_j-\omega_0|\ll\omega_0$. In this case, the mode propagation constants may be expanded as $p_{\ell,m}(\omega_j)=p_{\ell,m}(\omega_0)+p'_{\ell,m}(\omega_j-\omega_0)+0.5p''_{\ell,m}(\omega_j-\omega_0)^2$. According to Eqs. (3) and (4), FWM processes within a single transverse mode have a mismatch $\delta p_{\ell,m}=p''_{\ell,m}(\omega_1-\omega_3)(\omega_1-\omega_4)$. Now, the efficiency of FWM is strongly suppressed for mismatch

values larger than the inverse of the nonlinear length. As a result, the nonlinear spectral broadening of a light beam is restricted at long propagation distances [38]. When the interaction of different transverse modes is involved, the FWM mismatch may be equal to zero only occasionally, that is, for just a few quartets of waves. As a result, thermalization broadening of wave spectra fails to occur. Therefore, in the following we shall limit our treatment to pulses with a narrow spectrum ($\omega_k \simeq \omega$). As a matter of fact, in our experiments we use relative narrow-band picosecond pulses, whose spectral broadening is negligible over distances as long as z^*, which turns out to be of a few meters.

In the special case of GRIN fibers, the mode propagation constants are equidistant $p_{\ell,m} = p_{0,0} - n(2\pi/L_B)$, where $n = 2\ell + |m|$ is dubbed the quantum number, whereas L_B is the self-imaging distance. The condition of Eqs. (4) and (5) may be met for many quartets with $n_1 + n_2 = n_3 + n_4$ and $m_1 + m_2 = m_3 + m_4$ simultaneously. As a result, the ergodicity hypothesis is verified, and the equilibrium distribution [Eq. (2)] is achieved after a suitable nonlinear length: it can be written as

$$N_{\ell,m} = \frac{N_{0,0}}{1 - (2\pi V/L_B\tilde{\mu})(2\ell + |m|) + (\Omega/\tilde{\mu})m}, \quad (6)$$

where $\tilde{\mu} = \mu/\hbar\sqrt{2} + V p_{0,0} - \omega$. Note that the average power of transverse mode W_{lm} has the same distribution. In the Supplemental Material [34], we show that the FWM process in a multimode fiber can be described in the frame of a kinetic equation approach [10], for which the distribution [Eq. (6)] is found to be a stationary solution.

Importantly, Eq. (6) shows that the equilibrium RJ distribution is asymmetric with respect to $m = 0$, owing to the presence of the Lagrange's multiplier Ω, which is associated to the conservation of the total OAM [see Fig. 1(b), where $\Omega > 0$]. Specifically, the frequencies $(2\pi V/L_B)$ and Ω must be comparable, in order to significantly modify the symmetry of the RJ distribution around $m = 0$, whereas, if $\Omega = 0$, i.e., if the theory does not impose the conservation of the longitudinal OAM, then one recovers the conventional symmetric RJ distribution [12,23] [as in Fig. 1(a)]. Starting from this consideration, one can associate the presence of an OAM with the asymmetry of the mode distribution, i.e., with a nonzero value of the average azimuthal index $\langle m \rangle \propto \Omega$, where

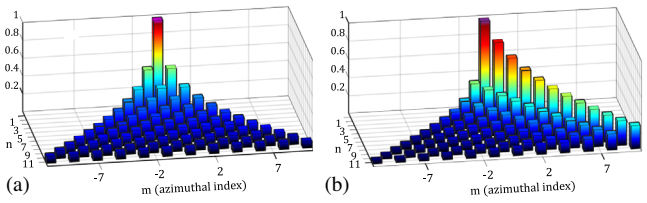

FIG. 1. Equilibrium distribution for $\Omega/\tilde{\mu} = 0$ (a) and $\Omega/\tilde{\mu} = -0.65$ (b). In both plots, $N_{0,0} = 1$ and $2\pi V/L_B\tilde{\mu} = 1$.

$$\langle m \rangle = \sum_{\ell,m} m W_{\ell,m}. \quad (7)$$

The symmetry breaking of the equilibrium distribution with respect to $m = 0$ means that, whenever thermalization without condensation ($\tilde{\mu} \neq 0$, i.e., when all the modes but the fundamental have $N_{\ell,m} = 0$) occurs, a bell-shaped output beam profile cannot be obtained, unless $\langle m \rangle = \Omega = 0$, in spite of the fact that the fundamental mode is always the dominant mode in the output thermal distribution. Experimentally, this means that, in order to achieve BSC, one always needs to inject a laser beam which does not carry OAM, e.g., on axis Gaussian beams, coupled at the center of the fiber core. It is worth pointing out that BSC was earlier demonstrated by using different input laser coupling configurations. This is the case of Ref. [9], where a diffuser changes the spatial distribution of the input beam, and of Ref. [21], where fiber was tilted with respect to the laser direction. However, in both of these cases no OAM was carried by the input beam.

In order to seed an OAM, we chose a peculiar input beam, i.e., a Gaussian beam which is injected with a tilt angle ϑ and a transverse offset y_0 with respect to the fiber axis [see Figs. 2(a) and 2(b)]. Such injection condition leads to helical propagation of the laser beam inside the fiber core [33,39]: its trajectory can be visualized by the naked eye by exploiting the luminescence of fiber defects [40]. The helical trajectory carries a longitudinal OAM, which can be calculated as

$$\langle m \rangle_{\text{the}} = 2\pi \frac{y_0 \sin\vartheta}{\lambda}. \quad (8)$$

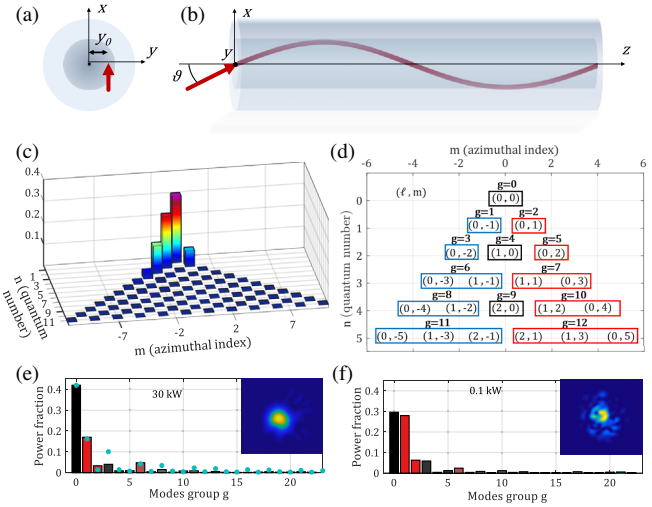

FIG. 2. (a),(b) Sketch of front and side views of injection conditions and helical propagation carrying positive OAM. (c) Input mode distribution. (d) Mode grouping by index g. (e) Numerically simulated output mode distribution when $W_p = 30$ kW. Cyan dots in the 2D plot represent the values of mode power fraction, obtained by fitting experimental data with Eq. (6). (f) Same as (e) when $W_p = 0.1$ kW. Images in the inset of (e) and (f) represent output intensity profiles of the beams.

Interestingly, the magnitude of the input OAM can be tuned by acting on the injection offset. Specifically, the input OAM grows larger with y_0, and its sign can be flipped by injecting the laser at diametrically opposite points, thus reversing the helix chirality [33]. Equation (8) was used to verify the validity of our mode truncation (see the Supplemental Material [34]).

In Fig. 2(c) we show the mode distribution at the input of the fiber, corresponding to the injection condition $\vartheta = 2°$ and $y_0 = -3$ μm. By applying Eq. (7), this corresponds to $\langle m \rangle = 0.75$ while $\langle n \rangle = \sum_{\ell,m}(2\ell + |m|)W_{\ell,m} = 2.23$.

In Fig. 2(d) we display a convenient way for grouping the OAM modes, which will be used in the remainder of this Letter. In this way, we can emphasize the difference between groups of modes, represented by number g: they share the same quantum number n, but have different signs of m. Specifically, modes with odd n are grouped in three blocks, one for $m < 0$, one for $m > 0$, and one of $m = 0$. On the other hand, modes with even n miss the value $m = 0$, so they are grouped in two blocks only, one for $m < 0$ and one for $m > 0$.

In order to verify the validity of our theoretical predictions, we performed numerical simulations. Besides FWM, we also considered the effects of linear random mode coupling [41]. Further details about the numerical model are reported in the Supplemental Material [34]. We limited our simulation to include the 78 modes with the highest values of momentum, i.e., we only considered GRIN fiber modes with $n < 12$.

We ran simulations for different values of the input peak power (W_p), in order to compare quasilinear with highly nonlinear propagation regimes. In the latter ($W_p = 30$ kW), the mode distribution at the output of the fiber [shown in Fig. 2(e)] turns out to be in excellent agreement with the generalized RJ distribution [Eq. (6)]. For a clearer comparison, we report in Fig. 2(e) the experimental (histogram) and fitting (cyan dots) values of the mode power fraction, whereas in the linear regime (i.e., for $W_p = 0.1$ kW), the lack of significant FWM interactions prevents mode thermalization: as a result, a fit with Eq. (6) fails [see Fig. 2(f)]. Details on simulation parameters are given in the Supplemental Material [34].

The validity of theory and numerics was verified by experiments based on the MD of OAM beams at the output of GRIN MMFs. The MD was performed by following the method described in Ref. [32]. We used 1 ps laser pulses at 1030 nm, and a 2 m long 50/125 GRIN MMF. A full description of the setup is reported in the Supplemental Material [34]. Here, we studied light thermalization, which is obtained by increasing the input pulse peak power, with two different injection conditions. Specifically, in Fig. 3, we report a MD analysis of the beam output profile for input beams carrying either positive [Figs. 3(a)–3(c)] or negative [Figs. 3(d)–3(f)] OAM. This was obtained by setting $y = +2$ μm or $y = -1$ μm, respectively. In the

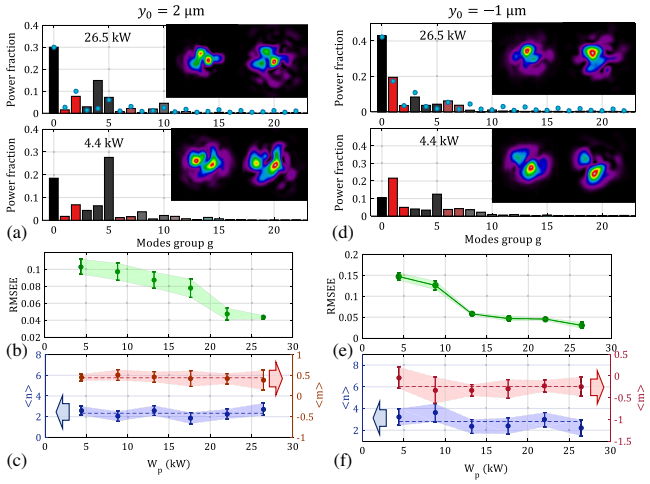

FIG. 3. Experimental results. (a) MD of the output beam for two different values of W_p, when $y_0 = +2$ μm. Inset: the measured output beam profiles (left) and their reconstructions (right). The blue dots are extracted by fitting experimental data with Eq. (6). (b) Root-mean-square error of the experimental mode distributions with respect to the generalized RJ distribution of Eq. (6) [cyan dots in (a)] vs input peak power. (c) Conservation of $\langle n \rangle$ (blue) and $\langle m \rangle$ (red). The error bars are estimated by considering all of the reconstructions of the output beam near field at each input power [12]. (d)–(f) Same as (a)–(c), when injecting the laser beam with an offset $y_0 = -1$ μm.

Supplemental Material [34], we also report the limit case of $\langle m \rangle = 0$, which is achieved by injecting the laser with no offset with respect to the fiber axis, whereas in the Supplemental Material [34] we provide more details on the evolution of mode occupancy toward thermalization, as the input beam power grows larger.

In Figs. 3(a) and 3(d), we report histograms of the mode power fraction of the output beams, for several values of W_p. As can be seen, the mode content changes when increasing W_p, eventually approaching an equilibrium distribution once overcoming the threshold for thermalization. One can appreciate that the distributions at $W_p = 17.6$ kW and $W_p = 26.5$ kW are quite similar, whereas at lower powers, significantly different output mode contents are observed. In the inset of Figs. 3(a) and 3(d), we compare the measured output near field intensities (images in the left column) with the MD reconstructions (images in the right column). These images are impressively similar for all input power values, thus proving the accuracy of our MD method.

The cyan dots shown in the graphs of Figs. 3(a) and 3(d) for the highest input power values provide the fitting of the experimental mode occupancy with Eq. (6). As can be seen, a good agreement is found between the experimental mode power fractions and the prediction of the generalized RJ distribution. In Figs. 3(b) and 3(e), we show that the root-mean-square error of the observed mode occupancy with respect to the equilibrium distribution is progressively reduced, when increasing W_p. This indicates that when

enough power is provided, the FWM processes allow for reaching the ergodicity condition for the multimode system, hence its thermalization into an equilibrium distribution; see Eq. (6).

Finally, we proved the validity of the hypothesis behind our theoretical derivation, i.e., the conservation laws of E, N, P, and M. As a matter of fact, our MD method does not allow for estimating $N_{\ell,m}$, since only averaged quantities can be extracted from camera pictures. Nevertheless, it is well known that the energy of each pulse E, and accordingly the photon number N, are conserved in our experimental conditions, since dissipative effects, of either linear or nonlinear origin, are negligible over a few meters of fiber for picosecond pulses of few tens of kW of peak power, at wavelengths around 1 μm. We experimentally verified the conservation of $\langle n \rangle$ and $\langle m \rangle$, which are related to the linear and angular momentum, respectively. As can be seen in Figs. 3(c) and 3(f), when varying W_p, both quantities oscillate within the experimental error bars around a constant value. Specifically, we found that $\langle m \rangle \simeq 0.46$ for $y_0 = +2\ \mu m$ and $\langle m \rangle \simeq -0.24$ for $y_0 = -1\ \mu m$. This is in agreement with theoretical expectations: Eq. (8) gives $\langle m \rangle = 0.44$ and $\langle m \rangle = -0.22$, respectively. We underline that increasing the fiber length or W_p is roughly equivalent, as far as nonlinear mode coupling in MMF is concerned [15,42]. Thus, the conservation of $\langle n \rangle$ and $\langle m \rangle$ with W_p also proves their conservation along the beam propagation distance.

In conclusion, we derived a general theoretical description of light thermalization in MMFs. Theoretical predictions have been confirmed by numerical and experimental studies. Remarkably, we found that the thermalization of OAM beams in GRIN MMFs may occur without the generation of bell-shaped output beams. Our work sheds new light on the nonlinear dynamics and manipulation of vortex optical beams by MMFs, which will have an echo in other areas of optics, e.g., for OAM-based optical trapping, and OAM-division-multiplexed telecommunications. After the submission of our manuscript, a theoretical study of OAM beam thermalization in multimode waveguides has been independently reported in Ref. [43].

This work was supported by the Russian Ministry of Science and Education (14.Y26.31.0017), the H2020 EU European Research Council (740355), and Ministero dell'Istruzione, dell'Università e della Ricerca (R18SPB8227). E. P., M. G., D. Kh., and S. B. were also supported by the Russian Science Foundation (21-72-30024).

*Corresponding author.
fabio.mangini@uniroma1.it
†These authors have contributed equally to this work.

[1] S. Dyachenko, A. Newell, A. Pushkarev, and V. Zakharov, Physica (Amsterdam) **57D**, 96 (1992).
[2] C. Connaughton, C. Josserand, A. Picozzi, Y. Pomeau, and S. Rica, Phys. Rev. Lett. **95**, 263901 (2005).
[3] A. Picozzi, J. Garnier, T. Hansson, P. Suret, S. Randoux, G. Millot, and D. Christodoulides, Phys. Rep. **542**, 1 (2014), optical wave turbulence: Towards a unified nonequilibrium thermodynamic formulation of statistical nonlinear optics.
[4] C. Sun, S. Jia, C. Barsi, S. Rica, A. Picozzi, and J. W. Fleischer, Nat. Phys. **8**, 470 (2012).
[5] D. R. Tilley and J. Tilley, *Superfluidity and Superconductivity* (Routledge, New York, 2019).
[6] H. Kondakci, A. F. Abouraddy, and B. E. Saleh, Nat. Phys. **11**, 930 (2015).
[7] H. E. Kondakci, A. Szameit, A. F. Abouraddy, D. N. Christodoulides, and B. E. Saleh, Optica **3**, 477 (2016).
[8] C. You, M. Hong, N. Bhusal, J. Chen, M. A. Quiroz-Juárez, J. Fabre, F. Mostafavi, J. Guo, I. De Leon, R. d. J. León-Montiel *et al.*, Nat. Commun. **12**, 1 (2021).
[9] K. Baudin, A. Fusaro, K. Krupa, J. Garnier, S. Rica, G. Millot, and A. Picozzi, Phys. Rev. Lett. **125**, 244101 (2020).
[10] P. Aschieri, J. Garnier, C. Michel, V. Doya, and A. Picozzi, Phys. Rev. A **83**, 033838 (2011).
[11] F. O. Wu, A. U. Hassan, and D. N. Christodoulides, Nat. Photonics **13**, 776 (2019).
[12] F. Mangini, M. Gervaziev, M. Ferraro, D. Kharenko, M. Zitelli, Y. Sun, V. Couderc, E. Podivilov, S. Babin, and S. Wabnitz, Opt. Express **30**, 10850 (2022).
[13] K. Krupa, A. Tonello, A. Barthélémy, V. Couderc, B. M. Shalaby, A. Bendahmane, G. Millot, and S. Wabnitz, Phys. Rev. Lett. **116**, 183901 (2016).
[14] K. Krupa, A. Tonello, A. Barthélémy, T. Mansuryan, V. Couderc, G. Millot, P. Grelu, D. Modotto, S. A. Babin, and S. Wabnitz, APL Photonics **4**, 110901 (2019).
[15] K. Krupa, A. Tonello, B. M. Shalaby, M. Fabert, A. Barthélémy, G. Millot, S. Wabnitz, and V. Couderc, Nat. Photonics **11**, 237 (2017).
[16] E. V. Podivilov, D. S. Kharenko, V. A. Gonta, K. Krupa, O. S. Sidelnikov, S. Turitsyn, M. P. Fedoruk, S. A. Babin, and S. Wabnitz, Phys. Rev. Lett. **122**, 103902 (2019).
[17] A. Fusaro, J. Garnier, K. Krupa, G. Millot, and A. Picozzi, Phys. Rev. Lett. **122**, 123902 (2019).
[18] E. Deliancourt, M. Fabert, A. Tonello, K. Krupa, A. Desfarges-Berthelemot, V. Kermene, G. Millot, A. Barthélémy, S. Wabnitz, and V. Couderc, OSA Continuum **2**, 1089 (2019).
[19] E. Deliancourt, M. Fabert, A. Tonello, K. Krupa, A. Desfarges-Berthelemot, V. Kermene, G. Millot, A. Barthélémy, S. Wabnitz, and V. Couderc, Opt. Express **27**, 17311 (2019).
[20] Y. Leventoux, A. Parriaux, O. Sidelnikov, G. Granger, M. Jossent, L. Lavoute, D. Gaponov, M. Fabert, A. Tonello, K. Krupa, A. Desfarges-Berthelemot, V. Kermene, G. Millot, S. Février, S. Wabnitz, and V. Couderc, Opt. Express **28**, 14333 (2020).
[21] M. Fabert, M. Săpânan, K. Krupa, A. Tonello, Y. Leventoux, S. Février, T. Mansuryan, A. Niang, B. Wetzel, G. Millot, S. Wabnitz, and V. Couderc, Sci. Rep. **10**, 20481 (2020).
[22] M. Zitelli, M. Ferraro, F. Mangini, and S. Wabnitz, Photonics Res. **9**, 741 (2021).

[23] Y. Wu, H. Pourbeyram, D. N. Christodoulides, and F. W. Wise, Opt. Lett. **46**, 3312 (2021).
[24] L. Allen, M. W. Beijersbergen, R. J. C. Spreeuw, and J. P. Woerdman, Phys. Rev. A **45**, 8185 (1992).
[25] J. Wang, J.-Y. Yang, I. M. Fazal, N. Ahmed, Y. Yan, H. Huang, Y. Ren, Y. Yue, S. Dolinar, M. Tur *et al.*, Nat. Photonics **6**, 488 (2012).
[26] R. Fickler, G. Campbell, B. Buchler, P. K. Lam, and A. Zeilinger, Proc. Natl. Acad. Sci. U.S.A. **113**, 13642 (2016).
[27] H. Oraizi and H. Emamian, Sci. Rep. **10**, 7358 (2020).
[28] Y. Bromberg, Y. Lahini, E. Small, and Y. Silberberg, Nat. Photonics **4**, 721 (2010).
[29] S. M. Block, Nature (London) **360**, 493 (1992).
[30] N. Simpson, L. Allen, and M. Padgett, J. Mod. Opt. **43**, 2485 (1996).
[31] H. Pourbeyram, P. Sidorenko, F. O. Wu, N. Bender, L. Wright, D. N. Christodoulides, and F. Wise, Nat. Phys. 1 (2022).10.1038/s41567-022-01579-y
[32] M. D. Gervaziev, I. Zhdanov, D. S. Kharenko, V. A. Gonta, V. M. Volosi, E. V. Podivilov, S. A. Babin, and S. Wabnitz, Laser Phys. Lett. **18**, 015101 (2020).
[33] F. Mangini, M. Ferraro, M. Zitelli, V. Kalashnikov, A. Niang, T. Mansuryan, F. Frezza, A. Tonello, V. Couderc, A. Aceves, and S. Wabnitz, Sci. Rep. **11**, 13030 (2021).
[34] See Supplemental Material at http://link.aps.org/supplemental/10.1103/PhysRevLett.128.243901 for additional details and background information.
[35] K. Krupa, A. Tonello, V. Couderc, A. Barthélémy, G. Millot, D. Modotto, and S. Wabnitz, Phys. Rev. A **97**, 043836 (2018).
[36] J. Lægsgaard, Opt. Lett. **43**, 2700 (2018).
[37] L. Landau and E. Lifshitz, in *Statistical Physics*, 3rd ed., edited by L. Landau and E. Lifshitz (Butterworth-Heinemann, Oxford, 1980), pp. 111–157.
[38] S. A. Babin, D. V. Churkin, A. E. Ismagulov, S. I. Kablukov, and E. V. Podivilov, J. Opt. Soc. Am. B **24**, 1729 (2007).
[39] F. Mangini, M. Ferraro, M. Zitelli, A. Niang, T. Mansuryan, A. Tonello, V. Couderc, A. De Luca, S. Babin, F. Frezza *et al.*, Opt. Lett. **47**, 1 (2022).
[40] F. Mangini, M. Ferraro, M. Zitelli, A. Niang, A. Tonello, V. Couderc, and S. Wabnitz, Phys. Rev. Applied **14**, 054063 (2020).
[41] O. S. Sidelnikov, E. V. Podivilov, M. P. Fedoruk, and S. Wabnitz, Opt. Fiber Technol. **53**, 101994 (2019).
[42] M. Ferraro, F. Mangini, M. Zitelli, A. Tonello, A. D. Luca, V. Couderc, and S. Wabnitz, Photonics Res. **9**, 2443 (2021).
[43] F. O. Wu, Q. Zhong, H. Ren, P. S. Jung, K. G. Makris, and D. N. Christodoulides, Phys. Rev. Lett. **128**, 123901 (2022).